

Electronic supplementary information (ESI)

Tuning the Plasmonic Resonance of Cu_{2-x}S

Nanocrystals: Effects of Crystal Phase, Morphology and Surface Ligands

Dongxu Zhu,^a Aiwei Tang,*^{ab} Lan Peng,^a Zhenyang Liu,^a Chunhe Yang,^a and
Feng Teng*^b

^a*Department of Chemistry, School of Science, Beijing JiaoTong University, Beijing 100044, China.*

E-mail: awtang@bjtu.edu.cn

^b*Key Laboratory of Luminescence and Optical Information, Ministry of Education, Beijing
JiaoTong University, Beijing 100044, China.*

Figure. S1

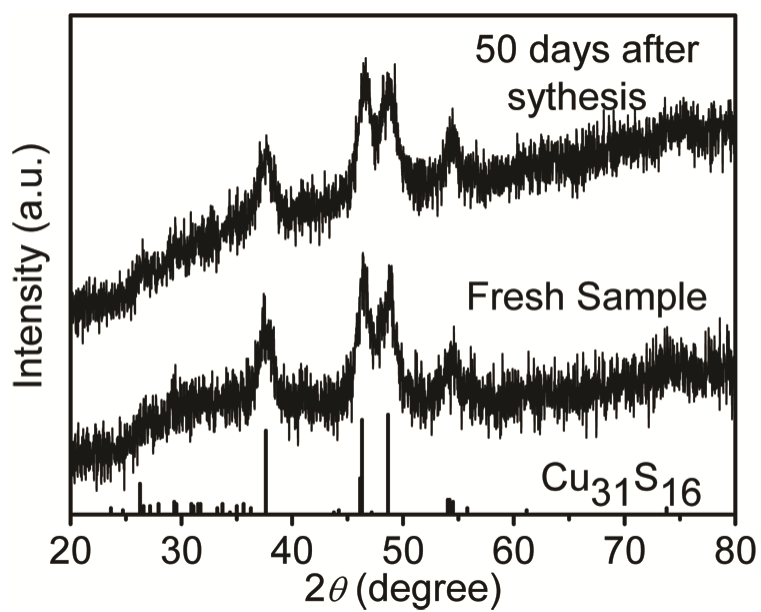


Fig.S1 XRD patterns of the product synthesized by using the Cu/S feeding ratio of 2:1, which were measured on the day of synthesis and after 50 days upon exposure to air.

Figure. S2

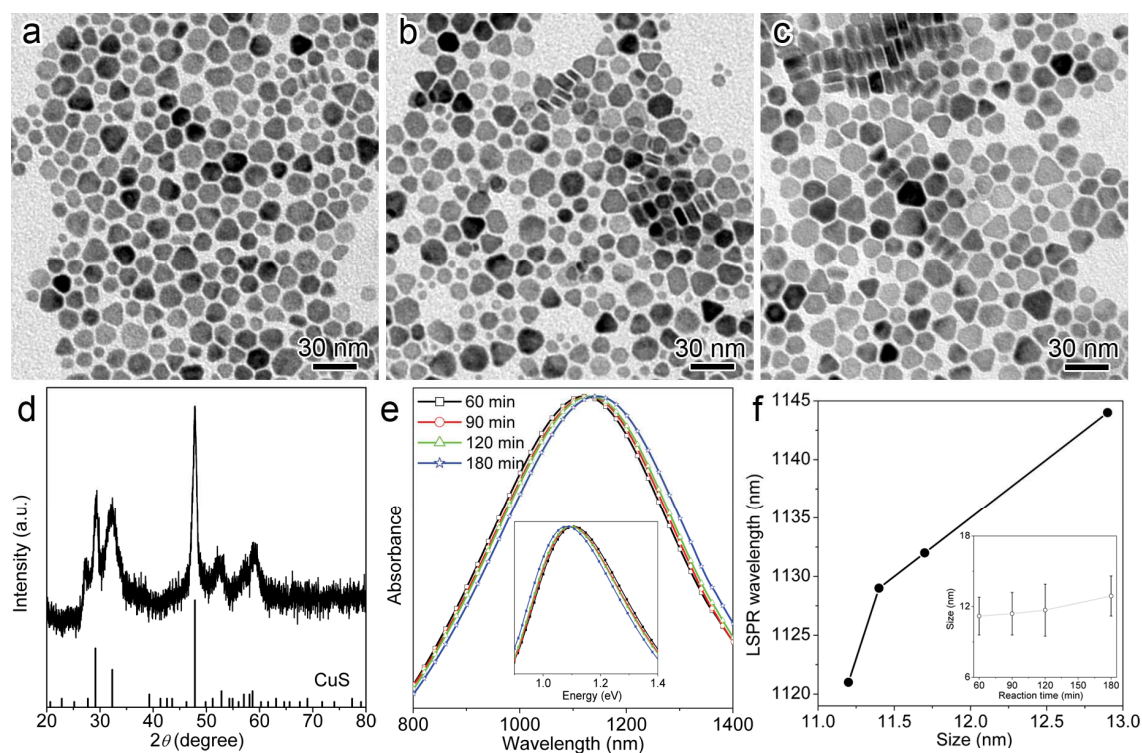


Fig.S2 TEM images of the as-obtained CuS nanodisks obtained at different reaction time: (a)60 min; (b) 90 min and (c) 180 min.(d) XRD patterns of the product obtained at 180 min, and the bottom lines represent the standard diffraction peaks of the hexagonal CuS (JCPDS No.06-0464); (e) LSPR absorption spectra on the wavelength scale of the products obtained for different reaction time, and the inset shows the corresponding LSPR spectra on the energy scale; (f) LSPR wavelength as a function of the average size, and the inset shows the average size versus the reaction time.

Figure. S3

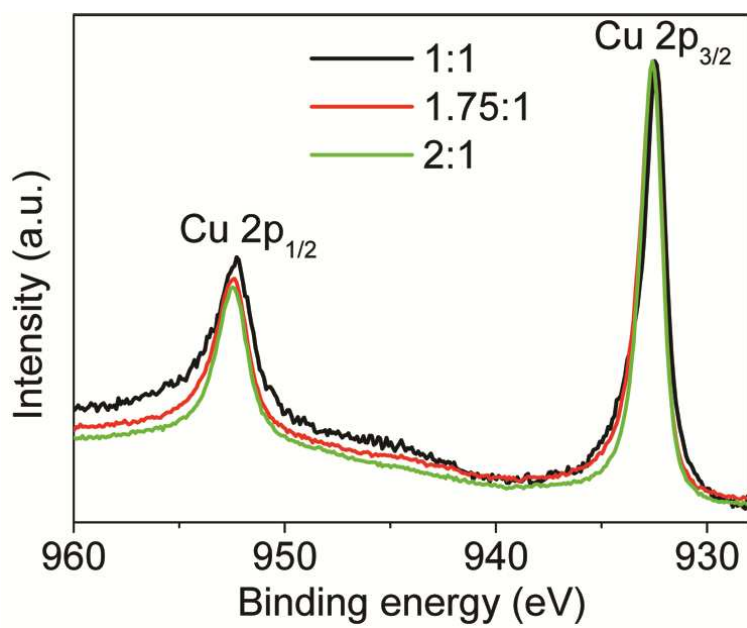


Fig.S3 XPS spectra of Cu 2p in the as-obtained products with different phases, and all the spectra were normalized.

Figure. S4

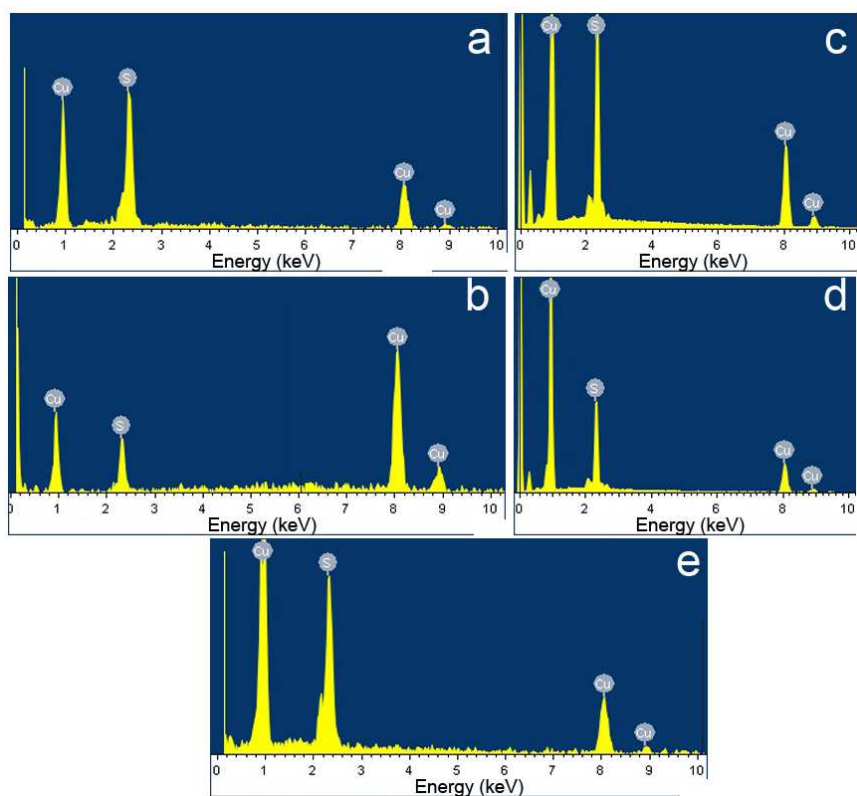


Fig.S4 EDS patterns of Cu_{2-x}S NCs synthesized by using different Cu/S feeding molar ratios: (a)1:1;(b)1.2:1;(c)1.4:1;(d)1.75:1;(e)2:1.

Figure. S5

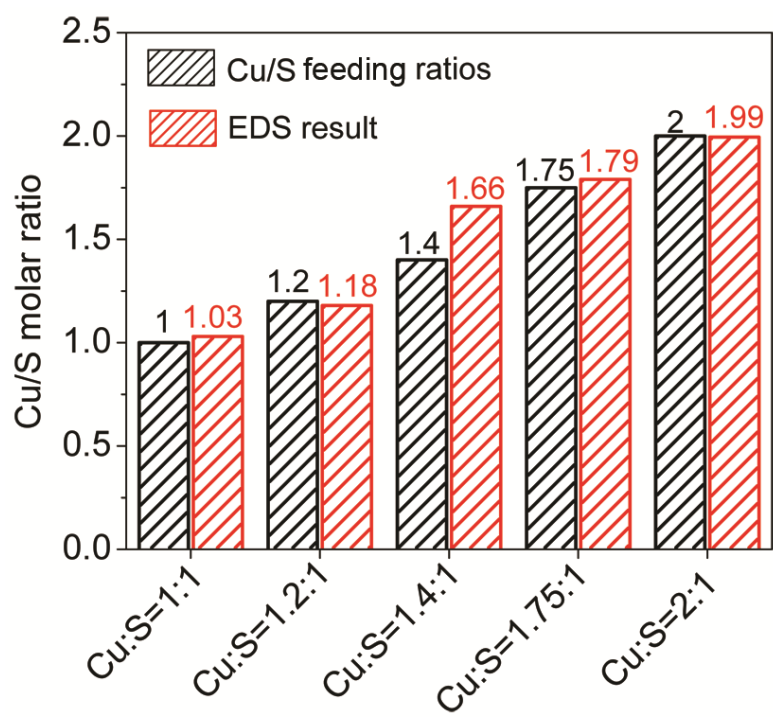


Fig.S5 The comparison of the Cu/S molar ratio between the feeding ratios and the EDS results for the different Cu_{2-x}S NCs synthesized by using the different Cu/S feeding ratios.

Figure. S6

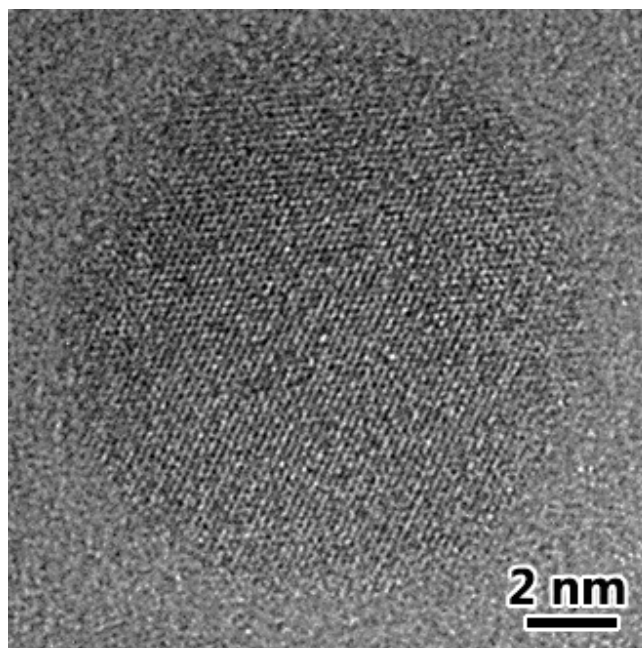


Fig.S6 The HRTEM images Cu_{2-x}S NCs synthesized by injection of S-OM precursors into Cu-OA:OM(1:1) precursors.

Figure. S7

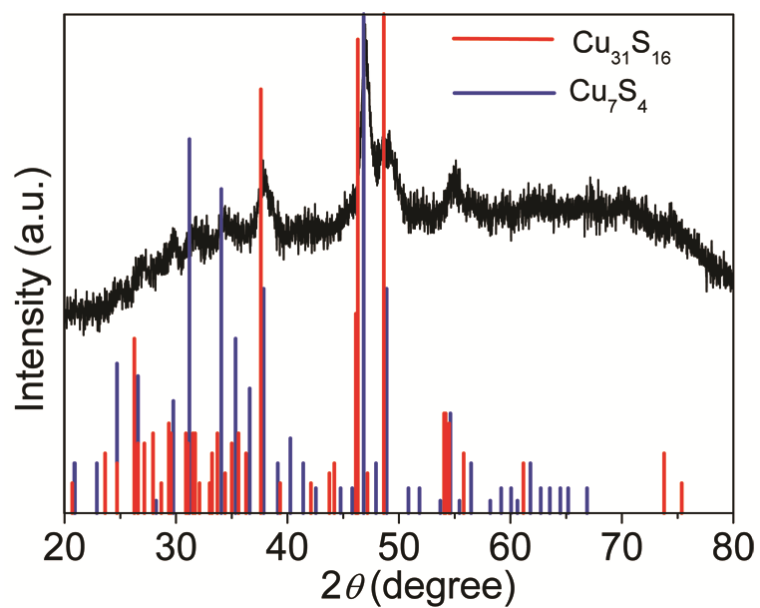


Fig.S7 XRD pattern of the products synthesized by injection S-OM into Cu-OM precursors, and the bottom vertical lines represent the standard diffraction peaks of monoclinic Cu_7S_4 (Roxbyite, JCPDS No.23-0958) and monoclinic $\text{Cu}_{31}\text{S}_{16}$ (Djureleite, JCPDS No.23-0959).

Figure. S8

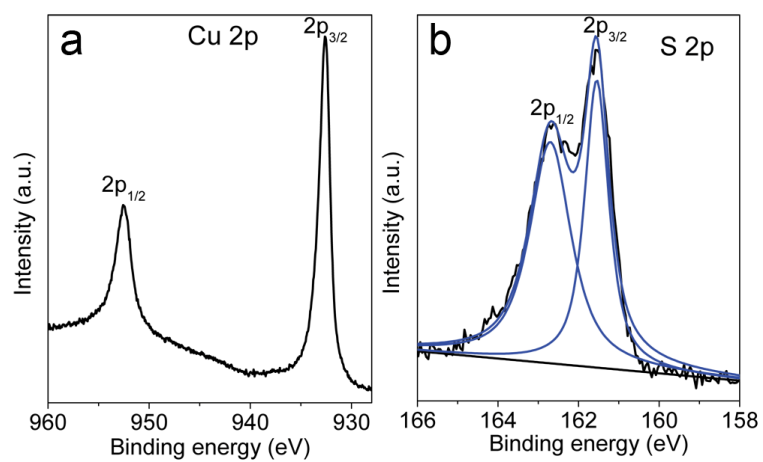


Fig.S8 High-resolution XPS spectra of (a) Cu 2p and (b) S 2p for the product synthesized by injection of S-OM into Cu-OM precursors.

Figure. S9

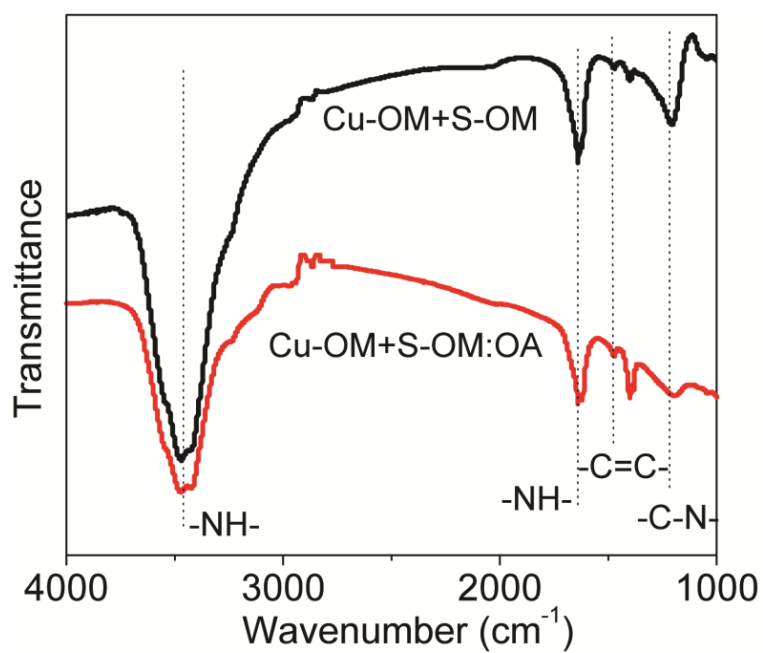


Fig.S9 FTIR spectra of the products synthesized by injection of S-OM and S-OA:OM(1:1) into the Cu-OM precursors.

Figure. S10

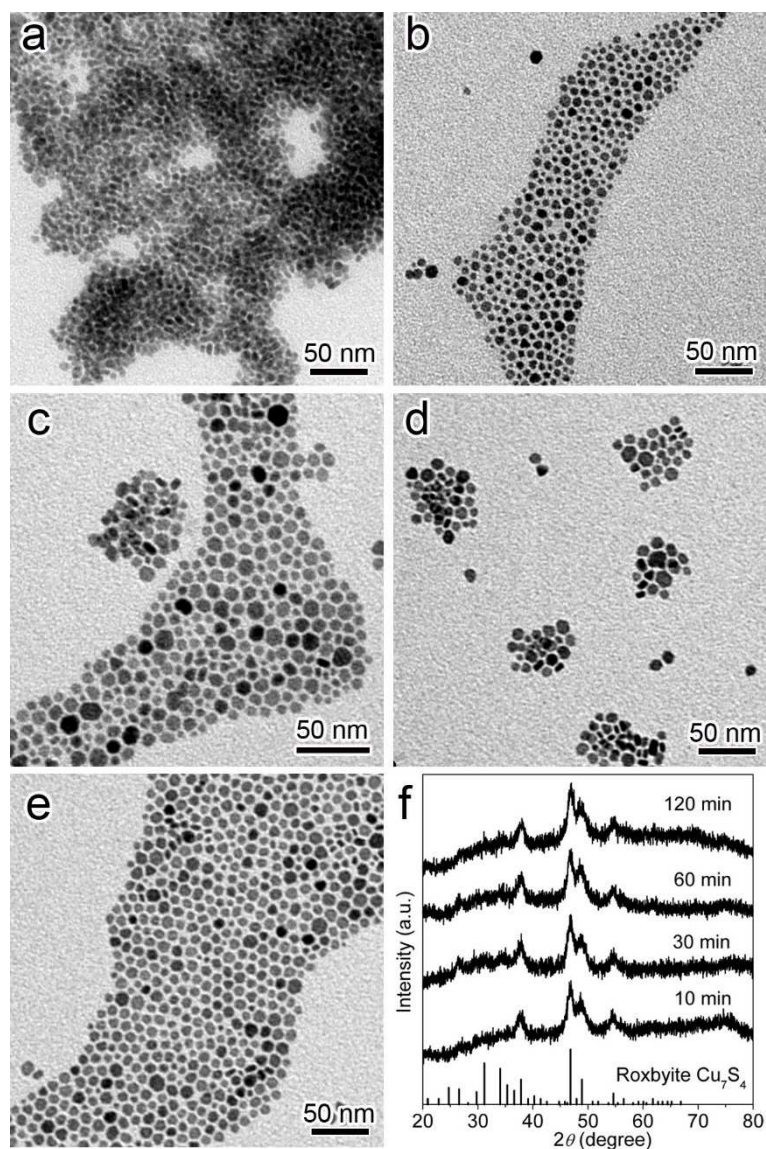


Fig.S10 TEM images of the products synthesized by injection of S-OA:OM (1:1) into the Cu-OA:OM(1:1) precursors for different reaction time: (a) 5 min; (b) 10 min; (c) 30 min; (d) 60 min; (e) 120 min; (f) XRD patterns of the products obtained at different reaction time, and the bottom lines are the standard diffraction peaks of monoclinic Cu₇S₄ (JCPDS 23-0958).

Figure. S11

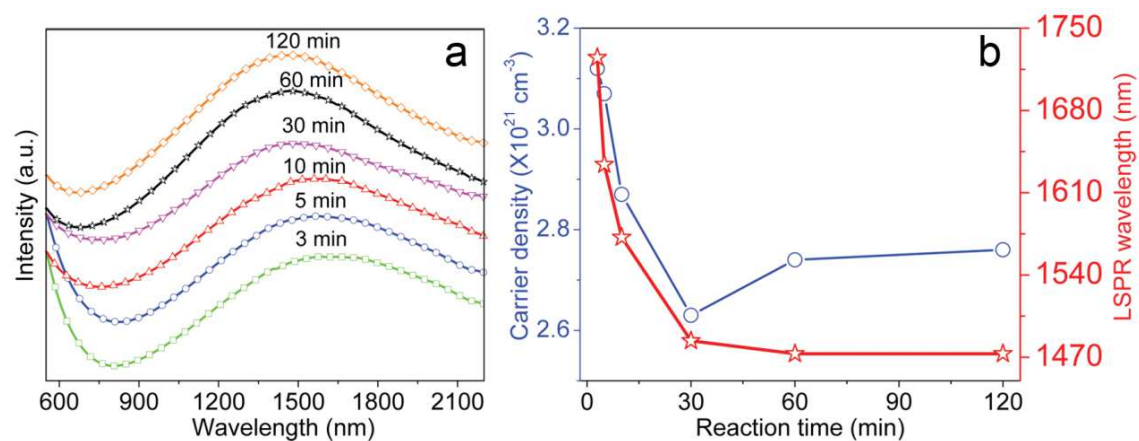


Fig.S11 (a) NIR LSPR absorption spectra of the products synthesized by injection of S-OA:OM(1:1) into the Cu-OA:OM(1:1) precursors for different reaction time; (b) The calculated carrier density and the LSPR wavelength as a function of reaction time.

Figure. S12

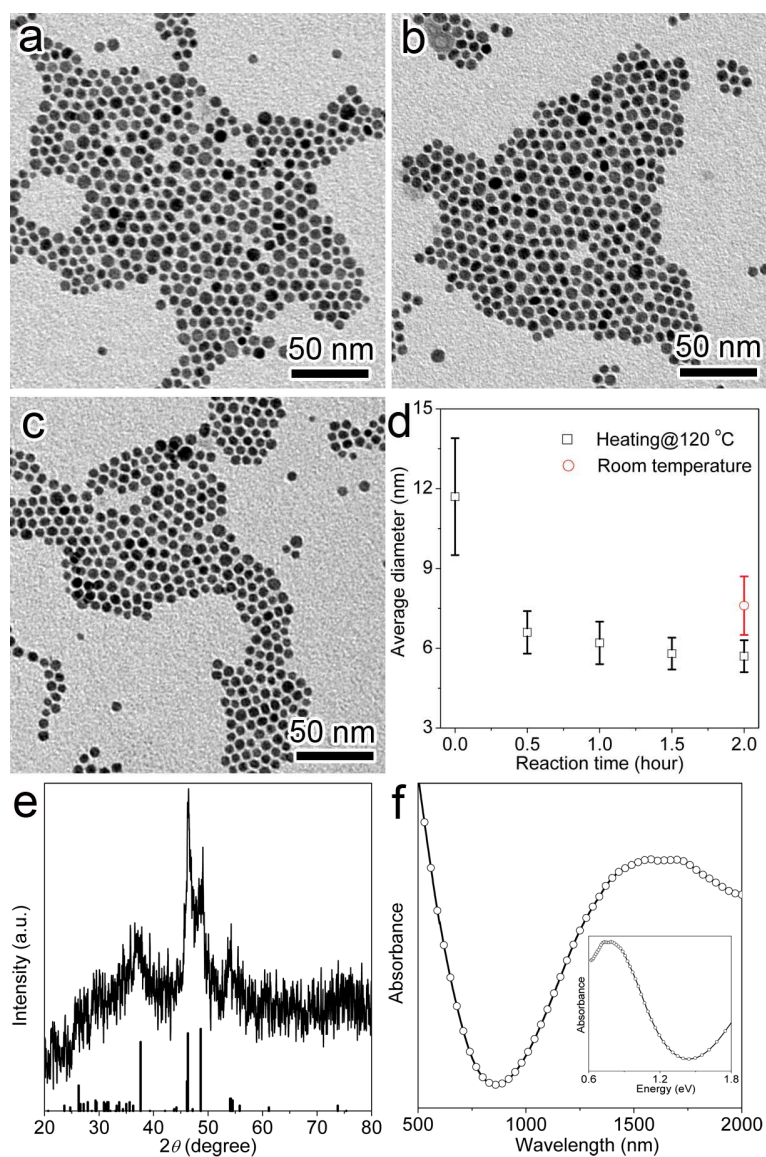


Fig.S12 TEM images of the products after post-treatment by DDT at 120 °C for different reaction time: (a) 30 min; (b) 60 min; (c) 90 min. (d) The average diameter of the products versus reaction time after post-treatment by DDT at room temperature and at 120 °C; (e) XRD patterns and (f) LSPR spectrum of the products after post-treatment at 120 °C for 30 min, and the inset of Figure (f) is the LSPR spectrum on the energy scale.

Figure. S13

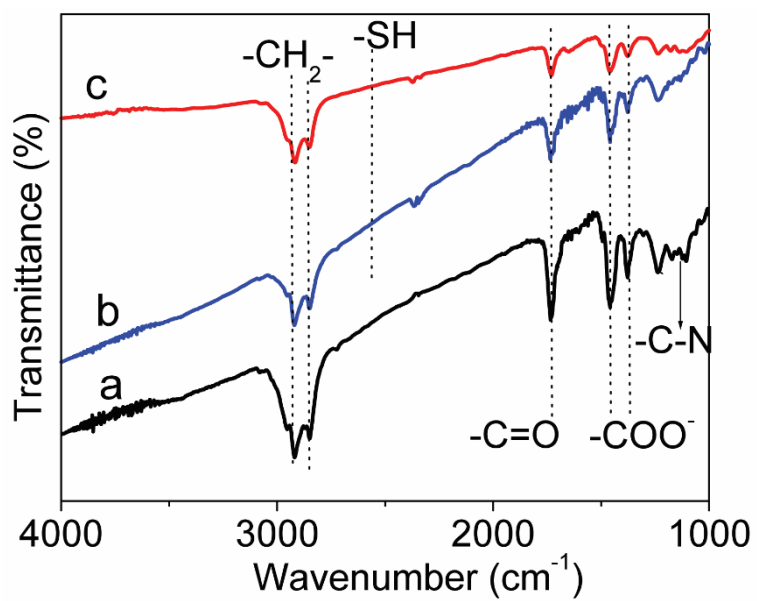


Fig.S13 FTIR spectra of the products (a) before and (b, c) after post-treatment by DDT: (b) at 120 °C and (c) room temperature for 2 h.